Temperature Dependence of the Excess Molar Heat Capacities for Alcohol−Alkane Mixtures. Experimental Testing of the Predictions from a Two-State Model

7 AUTHORS, INCLUDING:

Clara Asunción Tovar
University of Vigo
53 PUBLICATIONS   926 CITATIONS

SEE PROFILE

Enrique Carballo
University of Vigo
79 PUBLICATIONS   1,334 CITATIONS

SEE PROFILE

Miguel Costas
Universidad Nacional Autónoma de México
106 PUBLICATIONS   2,089 CITATIONS

SEE PROFILE

Temperature Dependence of the Excess Molar Heat Capacities for Alcohol−Alkane Mixtures. Experimental Testing of the Predictions from a Two-State Model

Claudio A. Cerdeiriña,[†] Clara A. Tovar,[†] Enrique Carballo,[†] Luis Romaní,*,[†] María del Carmen Delgado,[‡,§] Luis A. Torres,[‡] and Miguel Costas*,[‖]

Departamento de Física Aplicada, Facultad de Ciencias del Campus de Ourense, Universidad de Vigo E-32004, Spain, Departamento de Química, Centro de Investigación y Estudios Avanzados del I. P. N., Apdo. Postal 14-740, México D. F. 07000, México, and Laboratorio de Termofísica, Departamento de Física y Química Teórica, Facultad de Química, Universidad Nacional Autónoma de México, Cd. Universitaria, México DF 04510, México.

Received: June 19, 2001; In Final Form: September 25, 2001

A simple association model for alcohol−alkane mixtures, based on the idea that only two energy states are accessible to alcohol molecules in the pure and in the solution states, predicts complex temperature and alcohol concentration dependences of the excess molar heat capacity, $C_{p,m}^E$. These predictions are tested through the accurate measurement of pure component and solution heat capacities in the 278.15−338.15 K temperature interval. These measurements were performed at low, equimolar, and high alcohol concentrations for a linear alcohol (1-butanol) and a branched alcohol (3-methyl-3-pentanol) mixed with *n*-decane and with toluene. The qualitative predictions from the two-state model are corroborated by the data. According to this model, the very different $C_{p,m}^E$ behaviors found for the different systems arise simply through the change in hydrogen bonding Gibbs energy occurring on moving from the linear to the branched alcohol and in going from the inert *n*-decane to the aromatic toluene.

I. Introduction

The formation of hydrogen-bonded species between alcohol molecules in an inert solvent decreases the entropy of the system. These structures are broken up as the temperature increases producing an increase of entropy and heat capacity, $C_p = T (\delta S/\delta T)_p$. The heat capacity can then be used as an approximate indicator of molecular structure in the liquid mixture. At 298 K, the excess molar heat capacities, $C_{p,m}^E$, and also the excess molar enthalpies, H_m^E, are strongly positive; positive H_m^E reveals a net breaking of hydrogen bonds on mixing, but positive $C_{p,m}^E$ indicates more structure in the solution, so fewer hydrogen bonds in solution corresponds to bringing together alcohol molecules over longer distances than in the pure alcohol. Heat capacity measurements, both in the dilute alcohol concentration range and throughout the concentration range, have allowed the detailed study of the self-association of a variety of alcohols (linear, branched, cyclic, and aromatic) in inert solvents.[1−8] This heat capacity data, that in the majority of the cases has been obtained at 298 K, has been analyzed using an association model due to Treszczanowicz and Kehiaian.[9] Although it was not presented in such terms, this model is based on the idea that only two energy states are accessible to alcohol molecules in the pure and in the solution states.[10] This simple idea allows qualitative predictions of the temperature dependence of $C_{p,m}^E$ at different alcohol concentrations, providing an opportunity to study the changes in molecular structure in the liquid mixtures produced by temperature variations. In this work, these predictions are tested through the accurate measurement of the pure component and solution heat capacities in the 278−338 K temperature interval. These measurements were done at low, equimolar, and high alcohol concentrations for a linear alcohol (1-butanol) and a branched alcohol (3-methyl-3-pentanol) mixed with *n*-decane and with toluene.

II. Experimental Procedures and Results

Molar heat capacities in the 278.15−338.15 K temperature range were determined for pure components ($C_{p,m}^o$) and the following four mixtures ($C_{p,m}$): 1-butanol + *n*-decane, 1-butanol + toluene, 3-methyl-3-pentanol + *n*-decane, and 3-methyl-3-pentanol + toluene. Three concentrations were used in each case, namely, low alcohol concentration (mole fraction ca. 0.05), equimolar concentration, and high alcohol concentration (mole fraction ca. 0.95).

Materials. 1-butanol and toluene were from Fluka with 99.8+% purity. *n*-decane and 3-methyl-3-pentanol were from Sigma-Aldrich Chemical, Co., with 99+% purity. All chemicals were dried using 4 nm molecular sieves (from Fluka) and were degassed prior to use.

Procedures. Mixtures were prepared by weight using a Mettler AE-240 giving an accuracy of $\pm 5 \times 10^{-5}$ in the mole fractions. Volumetric heat capacities were measured with a differential scanning calorimeter Micro DSC II from Setaram, France, that has been described in detail in refs 11−14. The measurements were performed using the scanning method (0.5 K min^{-1}) that has been proved to be as accurate as the isothermal step method.[14] The calorimeter was calibrated employing *n*-heptane and 1-butanol whose heat capacities were taken from ref 15. Using this calorimeter, high sensitivity and

* To whom correspondence should be addressed. E-mail: romani@uvigo.es (L. Romaní) and costasmi@servidor.unam.mx (M. Costas).
† Universidad de Vigo.
‡ Centro de Investigación y Estudios Avanzados del I. P. N.
§ Present address: Unidad Queretaro del CINVESTAV, Apdo. Postal 1-708, Queretaro 76001, México.
‖ Universidad Nacional Autónoma de México.

TABLE 1: Molar Heat Capacities of the Pure Liquids

| | $C_{\mathrm{p,m}}^{\mathrm{o}}$/(J K^{-1} mol^{-1}) | | | | | |
| | *n*-decane | | toluene | | 3-methyl-3-pentanol | |
T/K	this work	ref 15	this work	ref 15	this work	ref 2
278.15	306.22	305.90	151.59	151.78	265.66	
280.65	307.30	306.87	152.21	152.42	270.93	
283.15	308.24	307.87	152.86	153.07	274.96	277.33
285.65	309.20	308.90	153.55	153.73	278.85	
288.15	310.18	309.95	154.22	154.39	282.73	
290.65	311.26	311.03	154.93	155.07	286.51	
293.15	312.37	312.13	155.65	155.75	290.19	
295.65	313.37	313.26	156.31	156.43	293.81	
298.15	314.49	314.41	157.02	157.13	297.31	302.25
300.65	315.62	315.58	157.71	157.83	300.67	
303.15	316.78	316.77	158.40	158.54	303.87	
305.65	318.02	317.98	159.20	159.25	306.83	
308.15	319.20	319.20	159.94	159.97	309.67	
310.65	320.39	320.44	160.65	160.69	312.39	
313.15	321.61	321.69	161.38	161.42	314.90	320.25
315.65	322.82	322.96	162.13	162.16	317.21	
318.15	324.16	324.24	162.94	162.90	319.27	
320.65	325.40	325.52	163.67	163.64	321.24	
323.15	326.66	326.82	164.38	164.39	323.06	332.75
325.65	327.93	328.12	165.09	165.15	324.67	
328.15	329.20	329.43	165.80	165.90	326.14	
330.65	330.54	330.75	166.57	166.67	327.39	
333.15	331.81	332.07	167.28	167.43	328.49	
335.65	333.09	333.39	167.93	168.20	329.51	
338.15	334.32	334.71	168.57	168.97	330.38	

optimum accuracy are reached when the working and reference cells are filled with liquids of similar volumetric heat capacities. For this reason, *n*-heptane was used in the reference cell when measuring the heat capacities of *n*-decane, toluene, the equimolar mixtures, and the low alcohol concentration mixtures. On the other hand, the reference cell was filled with 1-butanol when measuring the heat capacities of pure 3-methyl-3-pentanol and the high alcohol concentration mixtures. The volumetric heat capacities were transformed into molar heat capacities using the pure component and mixtures densities. These densities were determined using an Anton–Paar vibrating tube densimeter (model DSA-48) previously described[16] and calibrated using water and air. Densities were measured every 5° in the 278.15–338.15 K temperature range. With this procedure, the error is less than ± 5 × 10^{-5} g cm^{-3}. Cubic splines were used to fit the measured densities, so that the molar heat capacities can be calculated at any temperature within the 278.15–338.15 K temperature interval. The errors associated with the determination of the densities, and with the representation of these densities by cubic splines, do not affect significantly the accuracy of the molar heat capacities ($C_{\mathrm{p,m}}^{\mathrm{o}}$ and $C_{\mathrm{p,m}}$) that is estimated to be ± 0.05 J K^{-1} mol^{-1}. With this, the estimated accuracy of the excess molar heat capacities, $C_{\mathrm{p,m}}^{\mathrm{E}}$, is ± 0.1 J K^{-1} mol^{-1}. Heat capacities for pure components and their equimolar mixtures were also measured using a Perkin-Elmer DSC-7 calorimeter. Quantitatively, the results were slightly different from those presented here, with the qualitative behavior being fully analogous to that discussed below. Here, we only present the results obtained with the Micro DSC II because the comparison against literature values[11,12,15] showed that they are of higher quality.

Results. Table 1 shows the pure component molar heat capacities, $C_{\mathrm{p,m}}^{\mathrm{o}}$, compared against literature values.[2,15] 1-butanol is not included in this table because, as mentioned above, this alcohol was used as one of the calibrating liquids. The scanning method used to measure the heat capacities and the accuracy of our density determinations allow us to report $C_{\mathrm{p,m}}^{\mathrm{o}}$

at any temperature within the 278.15–338.15 K interval. In Table 1, we have elected to report $C_{\mathrm{p,m}}^{\mathrm{o}}$ every 2.5 degrees. For *n*-decane and toluene, the literature values in Table 1 are from the data-representation equations (cubic splines/quasipolynomium) reported in ref 15 that, in turn, are the result of a careful evaluation of all of the existing data. From Table 1, the average relative deviations between the present data and those in the literature are 0.06 and 0.08% for *n*-decane and toluene, respectively. This excellent agreement is a clear indication that the calorimeter employed and the procedures used are highly trustworthy. For 3-methyl-3-pentanol in Table 1, the present data are an improvement over the less accurate literature data.[2] Using the data in Table 1 together with the measurements of the molar heat capacities for the twelve mixtures studied in this work, the corresponding excess molar heat capacities $C_{\mathrm{p,m}}^{\mathrm{E}}$ were calculated and are reported in Table 2. For 1-butanol + *n*-decane and + toluene, it is possible to compare the data in Table 2 with literature values at 298.15 and 323.15 K, as shown in Table 3. As in the pure component case, the agreement is excellent, confirming that our calorimeter and experimental techniques produce reliable data. The pure component and excess heat capacity data in Tables 1 and 2 can be correlated using cubic splines of the form

$$X/(\mathrm{J\ K^{-1}\ mol^{-1}}) = \sum_{i=0}^{3} B_i T^i \qquad (1)$$

where X represents either $C_{\mathrm{p,m}}^{\mathrm{o}}$ or $C_{\mathrm{p,m}}^{\mathrm{E}}$. The B_i coefficients were obtained using the Marquardt algorithm[17] and are shown, together with the standard deviation of fit, in Table 4. For pure 3-methyl-3-pentanol, a better data representation was found using two temperature intervals.

III. Discussion

Two-State Model for Alcohol Molecules. It is assumed that each alcohol molecule, in the pure liquid and in an alcohol + inert mixture, is capable of two energy levels corresponding to the associated state (A_i) and the dissociated monomer (A).[10] This is indicated in Figure 1a where the associational energy of the system U(assoc) is shown as a function of $RT/|\Delta G^{\mathrm{o}}|$, the ratio of the thermal energy to the hydrogen bonding Gibbs energy ΔG^{o}, which is assumed to be temperature independent. In Figure 1, room temperature corresponds to a temperature where most of the alcohol molecules will still be associated. For a pure alcohol, at very low temperature U(assoc) will be low because all of the alcohol molecules will be associated through hydrogen bonds; as the temperature is raised, U(assoc) will rise corresponding to dissociation of the hydrogen bonds until, at high temperature, all alcohol molecules will be dissociated and in the form of monomers. For an alcohol + inert mixture, there is a greater entropic driving force toward the randomly dispersed alcohol molecules, and hence, it will be easier to break up hydrogen bonds, displacing U(assoc) as indicated in Figure 1a. In this context, an inert substance is one that does not interfere with the alcohol self-association, such as an *n*-alkane. According to Figure 1a, the associational contribution to the excess enthalpy (H^{E}(assoc) = U^{E}(assoc) at $P \cong 0$) for the mixing process is always positive. Taking the slope of the energy curves, *i.e. dU*-(*assoc*)/*dT* ($H = U$ at $P \cong 0$), the associational heat capacity for the pure alcohol $C_{\mathrm{p}}^{\mathrm{o}}$ and the mixture $C_{\mathrm{p}}^{\mathrm{mix}}$ are obtained as shown in Figure 1b. Note that, according to Figure 1b, it is possible that within the temperature range where the pure components and the mixtures are in the liquid state the

TABLE 2: Excess Molar Heat Capacities $C_{p,m}^E$ of x Alcohol + $(1 − x)$ Alkane

	$C_{p,m}^E$/ (J K^{-1} mol^{-1})											
	x 1-butanol + $(1 − x)$ n-decane			x 1-butanol + $(1 − x)$ toluene			x 3-methyl-3-pentanol + $(1 − x)$ n-decane			x 3-methyl-3-pentanol + $(1 − x)$ toluene		
							x					
T/K	0.05250	0.48952	0.94870	0.05014	0.50124	0.94938	0.05002	0.49595	0.94961	0.04962	0.49381	0.94881
278.15	7.14	9.62	1.26	6.50	13.46	1.96	10.32	15.63	1.80	3.64	16.47	2.53
280.65	7.62	10.29	1.33	6.43	13.94	2.01	10.31	16.17	1.83	2.98	15.95	2.41
283.15	7.94	10.87	1.43	6.32	14.22	2.07	10.02	16.94	1.90	2.40	15.49	2.33
285.65	8.22	11.42	1.49	6.18	14.49	2.12	9.63	17.76	2.14	1.86	14.98	2.29
288.15	8.52	11.98	1.64	6.04	14.76	2.20	9.19	18.47	2.26	1.32	14.41	2.20
290.65	8.89	12.57	1.79	5.91	15.00	2.31	8.68	19.08	2.44	0.86	13.72	2.15
293.15	9.18	13.14	1.92	5.72	15.23	2.40	8.09	19.65	2.56	0.39	12.99	2.02
295.65	9.53	13.76	2.03	5.49	15.47	2.46	7.37	20.21	2.69	−0.05	12.29	1.91
298.15	9.82	14.41	2.15	5.25	15.68	2.50	6.66	20.72	2.80	−0.49	11.50	1.83
300.65	10.05	15.06	2.27	5.00	15.89	2.57	5.92	21.23	2.95	−0.87	10.69	1.73
303.15	10.26	15.70	2.39	4.74	16.07	2.64	5.10	21.55	3.03	−1.23	9.85	1.59
305.65	10.48	16.33	2.56	4.55	16.21	2.76	4.33	21.72	3.14	−1.47	8.91	1.51
308.15	10.62	16.99	2.72	4.27	16.32	2.80	3.54	21.87	3.24	−1.75	7.98	1.27
310.65	10.69	17.65	2.81	4.00	16.47	2.86	2.76	21.89	3.30	−2.04	7.07	1.18
313.15	10.76	18.36	2.97	3.73	16.57	2.89	2.02	21.86	3.35	−2.25	6.15	1.00
315.65	10.71	18.90	3.09	3.42	16.61	2.95	1.31	21.68	3.40	−2.43	5.20	0.81
318.15	10.61	19.53	3.27	3.21	16.59	3.04	0.68	21.28	3.36	−2.53	4.20	0.66
320.65	10.42	20.17	3.40	2.92	16.61	3.08	0.07	20.97	3.42	−2.71	3.26	0.68
323.15	10.20	20.77	3.51	2.65	16.59	3.08	−0.51	20.52	3.41	−2.84	2.41	0.30
325.65	9.84	21.35	3.60	2.34	16.52	3.09	−1.02	19.98	3.40	−2.97	1.50	0.16
328.15	9.41	21.88	3.72	2.03	16.43	3.07	−1.46	19.31	3.39	−3.10	0.58	−0.04
330.65	8.91	22.30	3.85	1.80	16.24	3.13	−1.89	18.40	3.31	−3.16	−0.36	−0.14
333.15	8.33	22.65	3.97	1.51	16.01	3.13	−2.23	17.52	3.29	−3.25	−1.26	−0.29
335.65	7.70	23.10	4.07	1.18	15.83	3.12	−2.60	16.57	3.18	−3.39	−2.13	−0.36
338.15	6.95	23.47	4.15	0.84	15.50	3.06	−2.95	15.52	3.08	−3.52	−2.99	−0.44

TABLE 3: Comparison between the Excess Molar Heat Capacities, $C_{p,m}^E$, of This Work against Literature Values for x 1-butanol + $(1 − x)$ n-decane and + $(1 − x)$ Toluene

		$C_{p,m}^E$ J K^{-1} mol^{-1}			
		$T = 298.15$ K		$T = 323.15$ K	
mixture	x	this work	lit.	this work	lit.
	0.05250	9.82	9.57	10.20	9.29
1-butanol + n-decane[a]	0.48952	14.41	14.24	20.77	20.06
	0.94870	2.15	2.07	3.51	3.13
	0.05014	5.25	4.81	2.65	2.39
1-butanol + toluene[b]	0.50124	15.68	15.50	16.59	16.17
	0.94938	2.50	2.64	3.08	2.76

[a] Literature data from ref 11. [b] Literature data from ref 12.

associational heat capacity and hence the total heat capacity can go through a maximum. This prediction has been experimentally corroborated for some pure alcohols and will be reported in a forthcoming paper, together with an statistical mechanical treatment of the two-state model.[18]

The excess molar heat capacity is then given by

$$C_{p,m}^E = x[C_p^{mix}(assoc) − C_p^o(assoc)] \qquad (2)$$

where x is the alcohol mole fraction. In eq 2, only that part of the heat capacity that is due to association is taken into account because the internal heat capacity of the alcohol is eliminated and other intermolecular contributions will be small. According to eq 2, $C_{p,m}^E$ is simply given by the subtraction of the two curves in Figure 1b producing the behavior displayed in Figure 1c, where $C_{p,m}^E$ and $dC_{p,m}^E/dT$ are seen to change sign with temperature for a given system (a given $|\Delta G^o|$ value) or in going from one system to another (different $|\Delta G^o|$ values) at constant temperature. As will be shown below in detail, this simple two-state model is able to predict the temperature dependence of

$C_{p,m}^E$ for all of the mixtures studied in this work. In fact, one of the most attractive features of Figure 1c is that it provides a general framework for consideration of both order-creation and order-destruction processes during mixing, as discussed in detail in ref 10.

**Linear and Branched Alcohols Mixed with *n*-Decane.** Compared to linear alcohols, the self-association capabilities of branched alcohols are diminished due to the steric hindrance over their hydroxyl group.[2] As a consequence, the absolute value of the hydrogen bonding Gibbs energy for branched (br-OH) alcohols is smaller than that for the linear (l-OH) 1-alcohols, i.e., $|\Delta G_{br−OH}^o| < |\Delta G_{l−OH}^o|$. Then, in the *same* experimental temperature interval, branched alcohol + inert and linear alcohol + inert mixtures will belong to different regions in Figure 1c, as indicated in Figure 2a for equimolar mixtures. The data for 1-butanol + *n*-decane and 3-methyl-3-pentanol + *n*-decane displayed in Figure 2b with the data in Table 2 show that, at equimolar concentration, for a linear alcohol + *n*-alkane $C_{p,m}^E > 0$ with $dC_{p,m}^E/dT > 0$, whereas for a branched alcohol + *n*-alkane, $C_{p,m}^E > 0$ but with $dC_{p,m}^E/dT$ changing sign from positive to negative as the temperature increases. Thus, the model predictions regarding the change in $C_{p,m}^E$ and $dC_{p,m}^E/dT$ behavior in going from a linear to a branched alcohol are clearly corroborated by the experimental results.

Linear and Branched Alcohols Mixed with Toluene. When *n*-decane is substituted by toluene, the alcohol self-association is affected by π-hydrogen bonding characteristics of toluene. This interference with the alcohol self-association is due to the negative electron density in the aromatic ring of toluene that, in principle, is able to form weak hydrogen bonds with the acidic hydrogen of the alcohol hydroxyl group. Hydrogen bonds between an aromatic ring and an acidic hydrogen have been experimentally and theoretically found, for example, in mixtures of benzene with water.[19−22] Because these alcohol−toluene complexes are quite weak, the effect of the not-truly-inert
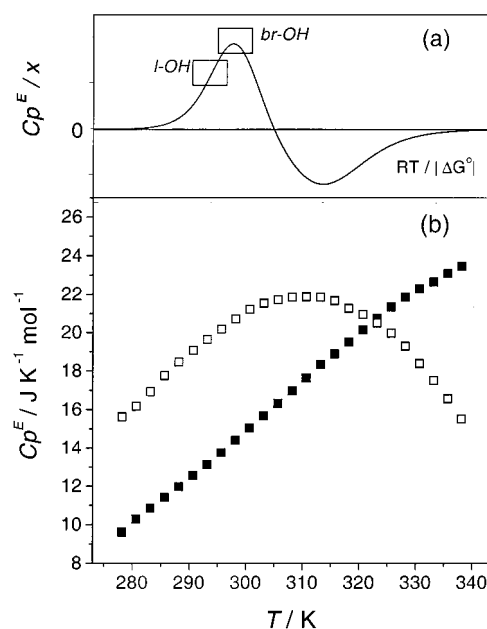
TABLE 4: Coefficients B_i of Eq 1 and Standard Deviations of Fit σ for Pure Components and x Alcohol + (1-x) Alkane Mixtures

		i				σ
pure liquid		0	1	2	3	
n-decane		746.40	−4.7268	0.015619	-1.5507×10^{-5}	0.05
toluene		474.53	−3.5947	0.012433	-1.3242×10^{-5}	0.04
3-methyl-3-pentanol (278.15−303.15)		684.08	−9.2522	0.044410	-5.9466×10^{-5}	0.04
3-methyl-3-pentanol (303.15−338.15)		−2564.5	21.146	−0.050022	3.7866×10^{-5}	0.04
n-heptane[a]		212.33	−0.3522	0.00155	-7.5025×10^{-7}	0.003
1-butanol[a]		653.71	−5.1277	0.01599	-1.3925×10^{-5}	0.04

		i				σ
mixture	x	0	1	2	3	
1-butanol + *n*-decane	0.05250	1277.8	−1.3633	0.048305	-5.6491×10^{-5}	0.04
	0.48952	919.05	−9.4422	0.031940	-3.5041×10^{-5}	0.06
	0.94870	212.02	−2.1480	0.0071481	-7.7296×10^{-6}	0.03
1-butanol + toluene	0.05014	−367.54	3.6340	−0.011500	1.1756×10^{-5}	0.04
	0.50124	423.31	−4.66240	0.017243	-2.0764×10^{-5}	0.02
	0.94938	182.46	−189.81	0.0065604	-7.4407×10^{-6}	0.03
3-methyl-3-pentanol + *n*-decane	0.05002	−2670.1	2.6729	−0.088015	9.5511×10^{-5}	0.10
	0.49595	557.85	−7.4822	0.031505	-4.1764×10^{-5}	0.10
	0.94961	122.32	−1.5122	0.0059529	-7.4636×10^{-6}	0.02
3-methyl-3-pentanol + toluene	0.04962	733.25	−6.3166	0.018111	-1.7370×10^{-5}	0.05
	0.49381	−1386.01	13.864	−0.044757	4.6878×10^{-5}	0.05
	0.94881	−465.34	4.5458	−0.014562	1.5332×10^{-5}	0.04

[a] From ref 15, used as calibrating liquids.
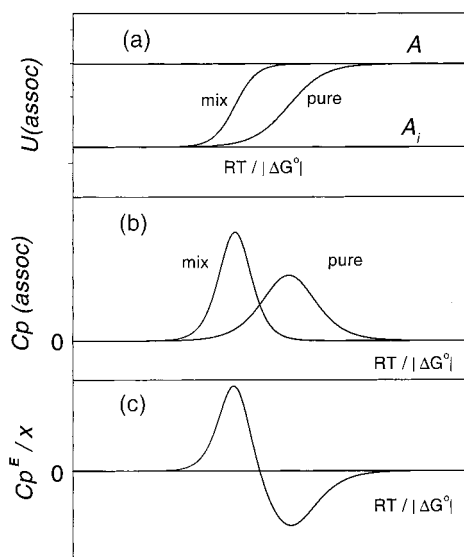
Figure 1. Schematic representation of (a) the associational energy U(assoc) and (b) associational heat capacity C_p(assoc) against $RT/|\Delta G^o|$ for an alcohol in the pure state (pure) and for an alcohol + inert mixture (mix). The two energy levels correspond to the associated state (A_i) and the dissociated monomer (A), and $RT/|\Delta G^o|$ is the ratio of the thermal energy to the hydrogen bonding Gibbs energy. Using eq 2, from the C_p(assoc) curves in b, the excess molar heat capacity divided by the alcohol mole fraction, $C_{p,m}^E/x$, is obtained (c).

Figure 2. (a) Schematic representation of $C_{p,m}^E/x$ against $RT/|\Delta G^o|$. Marked regions represent the expected behavior for a linear alcohol (l-OH) + inert mixture and for a branched alcohol (br-OH) + inert mixture. (b) Experimental $C_{p,m}^E$ from Table 2 for 1-butanol + *n*-decane (■) and for 3-methyl-3-pentanol + *n*-decane (□) at equimolar concentration.

toluene is basically the reduction of the alcohol self-association. Then, the net effect of toluene is to decrease the absolute value of the hydrogen bonding Gibbs energy for both linear and branched alcohol, i.e., $|\Delta G_{l-OH}^o(\text{tol})| < |\Delta G_{l-OH}^o(nC_n)|$ and $|\Delta G_{br-OH}^o(\text{tol})| < |\Delta G_{br-OH}^o(nC_n)|$. This implies that, in the *same* experimental temperature interval and with respect to the situation with the truly inert *n*-decane, linear alcohol + toluene and branched alcohol + toluene mixtures will be displaced to the right in the horizontal axis of Figure 2a, as indicated in Figure 3a for equimolar mixtures. The two-state model then predicts that for a linear alcohol + toluene $C_{p,m}^E > 0$ with

$dC_{p,m}^E/dT$ changing sign from positive to negative as the temperature increases, whereas for a branched alcohol + toluene $C_{p,m}^E$ would be positive at low temperatures and negative high temperatures with $dC_{p,m}^E/dT < 0$. The data in Table 2 for 1-butanol + toluene and 3-methyl-3-pentanol + toluene confirm these predictions as shown in Figure 3b.

Alcohol Concentration Dependence. In dilute alcohol mixtures, there is a strong entropic driving force toward the randomly dispersed alcohol molecules. For these mixtures, compared to the situation at equimolar concentration, it is easier to break up hydrogen bonds as the temperature increases,
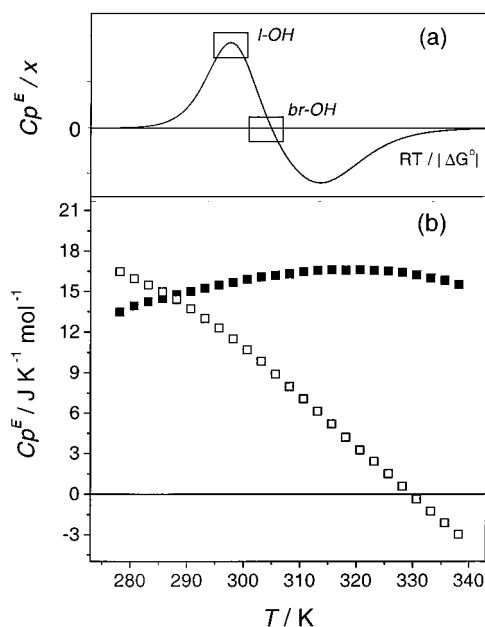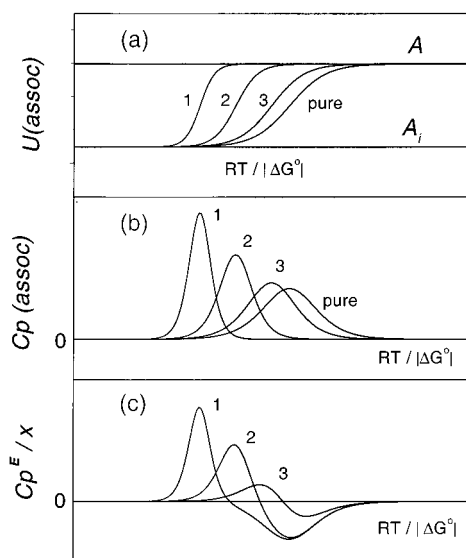
Molar Heat Capacities for Alcohol−Alkane Mixtures

J. Phys. Chem. B, Vol. 106, No. 1, 2002 **189**

Figure 3. (a) Schematic representation of $C_{p,m}^E/x$ against $RT/|\Delta G^\circ|$. Marked regions represent the expected behavior for a linear alcohol (l-OH) + noninert mixture and for a branched alcohol (br-OH) + noninert mixture. (b) Experimental $C_{p,m}^E$ from Table 2 for 1-butanol + toluene (■) and for 3-methyl-3-pentanol + toluene (□) at equimolar concentration.

Figure 5. (a) Schematic representation of $C_{p,m}^E/x$ against $RT/|\Delta G^\circ|$, at three alcohol concentrations. Marked regions represent the expected behavior for a linear alcohol + inert mixture at low (1), equimolar (2), and high (3) alcohol concentrations. (b) Experimental $C_{p,m}^E$ from Table 2 for 1-butanol + n-decane at low (□), equimolar (■), and high (▲) 1-butanol concentrations.

Figure 4. Schematic representation of (a) the associational energy U(assoc) and (b) associational heat capacity C_p(assoc) against $RT/|\Delta G^\circ|$ for an alcohol in the pure state (pure) and for an alcohol + inert mixture at low (1), equimolar (2), and high (3) alcohol concentrations. The two energy levels correspond to the associated state (A_i) and the dissociated monomer (A), and $RT/|\Delta G^\circ|$ is the ratio of the thermal energy to the hydrogen bonding Gibbs energy. Using eq 2, from the C_p(assoc) curves in b, the excess molar heat capacities divided by the alcohol mole fraction, $C_{p,m}^E/x$, at each alcohol concentration, are obtained (c).

displacing U(assoc) as indicated in Figure 4a. On the other hand, at high alcohol concentrations, U(assoc) is displaced toward the pure alcohol case. From these U(assoc) curves, the associational heat capacity for dilute and concentrated alcohol mixtures are obtained as shown in Figure 4b where the equimolar concentration and pure alcohol cases are also displayed. Using eq 2, the excess molar heat capacities for the different systems are then
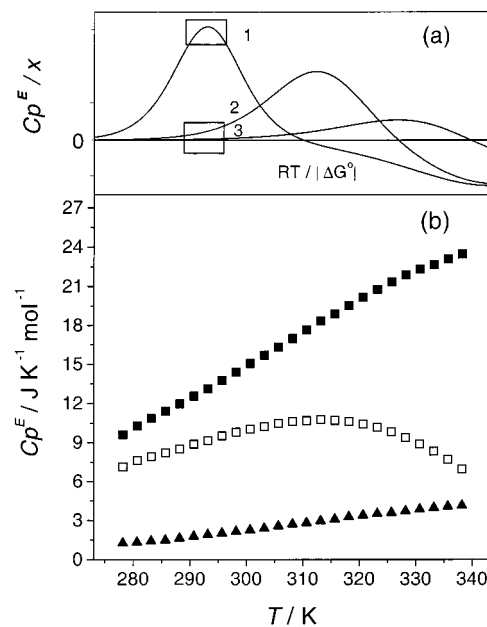
predicted to behave as shown in Figure 4c. For the linear 1-butanol mixed with n-decane, Figure 5a indicates these predictions, namely, at low alcohol concentration, $C_{p,m}^E > 0$ with $dC_{p,m}^E/dT$ changing sign from positive to negative as the temperature increases, whereas at high alcohol concentration, $C_{p,m}^E > 0$ and $dC_{p,m}^E/dT > 0$. The two-state model also predicts that at high alcohol concentration $dC_{p,m}^E/dT$ should be smaller than at equimolar concentration. Figure 5b show these predictions to be correct. Note that there is no disagreement between panels a and b in Figure 5 with respect to the magnitude of $C_{p,m}^E$, because in Figure 5a $C_{p,m}^E/x$ is plotted but in Figure 5b only $C_{p,m}^E$ is displayed. According to the two-state model, when 1-butanol is substituted by 3-methyl-3-pentanol, $C_{p,m}^E$ should follow the behavior shown in Figure 6a, owing to the smaller hydrogen bonding Gibbs energy for the branched alcohol as compared with the linear one. Again, the data in Table 2 supports these predictions as indicated in Figure 6b. Note that Figure 6a indicates that at high alcohol concentration the maximum for $C_{p,m}^E$ should occur at a higher temperature than for the equimolar mixture, a prediction that is also confirmed by the data in Figure 6b. As explained above, when n-decane is changed by toluene as the second component, the hydrogen bonding Gibbs energy is decreased. Then, for the *same* experimental temperature interval as with n-decane, for the two alcohols mixed with toluene, the different $C_{p,m}^E$ regions shown in Figures 5a and 6a will be displaced to the right in the horizontal axis, as indicated in Figures 7a and 8a. The two-state model predictions in these two panels are verified by the data shown in Figures 7b and 8b.

The comparison between panels a in Figures 2−8 (except Figure 4) shows that the change in $C_{p,m}^E$ behavior caused by the introduction of a steric hindrance on alcohol hydroxyl group, i.e., in going from 1-butanol to 3-methyl-3-pentanol, is qualitatively equivalent to changing the inert n-decane by toluene. This is due to a reduction of the self-association capabilities of

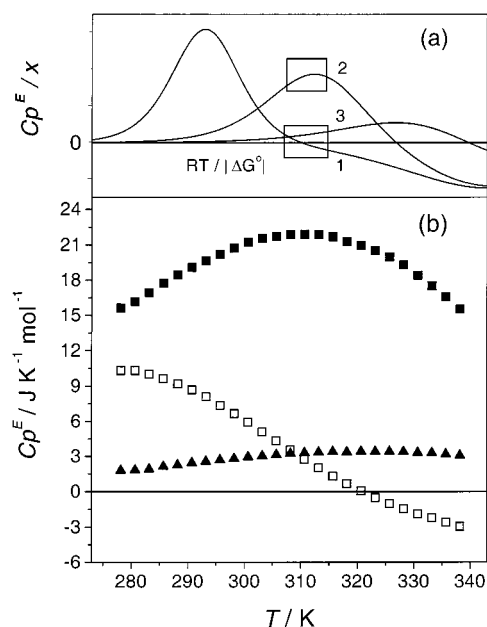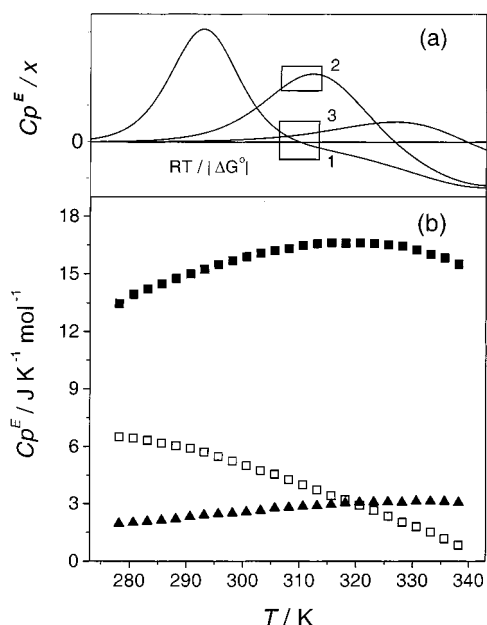**Figure 6.** (a) Schematic representation of $C_{p,m}^E/x$ against $RT/|\Delta G°|$, at three alcohol concentrations. Marked regions represent the expected behavior for a branched alcohol + inert mixture at low (1), equimolar (2), and high (3) alcohol concentrations. (b) Experimental $C_{p,m}^E$ from Table 2 for 3-methyl-3-pentanol + *n*-decane at low (□), equimolar (■), and high (▲) 3-methyl-3-pentanol concentrations.

Figure 7. (a) Schematic representation of $C_{p,m}^E/x$ against $RT/|\Delta G°|$, at three alcohol concentrations. Marked regions represent the expected behavior for a linear alcohol + noninert mixture at low (1), equimolar (2), and high (3) alcohol concentrations. (b) Experimental $C_{p,m}^E$ from Table 2 for 1-butanol + toluene at low (□), equimolar (■), and high (▲) 1-butanol concentrations.

the alcohol, a reduction that becomes more acute as the temperature increases. This effect is clearly seen for 3-methyl-3-pentanol + toluene. For this mixture, at low alcohol concentration, Table 2 and Figure 8b indicate that $C_{p,m}^E$ values are negative for most of the experimental temperature interval, and in fact, for $T > 330$ K, $C_{p,m}^E$ will probably be negative throughout the concentration range. The negative $C_{p,m}^E$ corresponds to a decrease in structure on passing from the pure
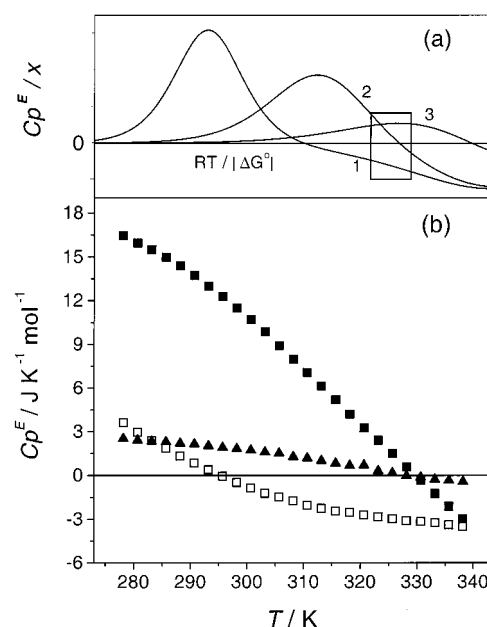

Figure 8. (a) Schematic representation of $C_{p,m}^E/x$ against $RT/|\Delta G°|$, at three alcohol concentrations. Marked regions represent the expected behavior for a branched alcohol + noninert mixture at low (1), equimolar (2), and high (3) alcohol concentrations. (b) Experimental $C_{p,m}^E$ from Table 2 for 3-methyl-3-pentanol + toluene at low (□), equimolar (■), and high (▲) 3-methyl-3-pentanol concentrations.

alcohol to the solution, implying that the mixture contains many alcohol monomers A and relatively few self-associated species A_i. Moreover, at $T \gg 330$ K, $dC_{p,m}^E/dT$ is expected to change sign from negative to positive (see Figure 1c). This model prediction could be tested by performing experiments at high temperatures; work in this direction is currently underway in our laboratories.

References and Notes

(1) Costas, M.; Patterson, D. *J. Chem. Soc., Faraday Trans. 1* **1985**, 81, 635.
(2) Caceres-Alonso, M.; Costas, M.; Andreoli-Ball, L.; Patterson, D. *Can. J. Chem.* **1988**, 66, 989.
(3) Andreoli-Ball, L.; Patterson, D.; Costas, M.; Caceres-Alonso, M. *J. Chem. Soc., Faraday Trans. 1* **1988**, 84, 3991.
(4) Andreoli-Ball, L.; Costas, M.; Paquet, P.; Patterson, D.; St. Victor, M. E. *Pure Appl. Chem.* **1989**, 61, 1075.
(5) Pérez-Casas, S.; Trejo, L. M.; Costas, M. *J. Chem. Soc., Faraday Trans.* **1991**, 87, 1733.
(6) Trejo, L. M.; Pérez-Casas, S.; Costas, M.; Patterson, D. *J. Chem. Soc., Faraday Trans.* **1991**, 87, 1739.
(7) Pérez-Casas, S.; Moreno-Esparza, R.; Costas, M.; Patterson, D. *J. Chem. Soc., Faraday Trans.* **1991**, 87, 1745.
(8) Figueroa-Gerstenmaier, S.; Cabañas, A.; Costas, M. *Phys. Chem. Chem. Phys.* **1999**, 1, 665.
(9) Kehiaian, H.; Treszczanowicz, A. J. *Bull. Acad. Chim. Fr.* **1969**, 5, 1561.
(10) Costas, M.; Patterson, D. *Thermochim. Acta* **1987**, 120, 181.
(11) Gates, J. A.; Wood, R. H.; Cobos, J. C.; Casanova, C.; Roux, A. H.; Roux-Desgranges, G.; Grolier, J.-P. E. *Fluid Phase Equilib.* **1986**, 27, 137.
(12) Cobos, J. C.; García, I.; Casanova, C.; Roux, A. H.; Roux-Desgranges, G.; Grolier, J.-P. E. *Fluid Phase Equilib.* **1991**, 69, 223.
(13) Tovar, C. A.; Carballo, E.; Cerdeiriña, C. A.; Legido, J. L.; Romaní, L. *Int. J. Thermophys.* **1997**, 18, 761.

Molar Heat Capacities for Alcohol−Alkane Mixtures

J. Phys. Chem. B, Vol. 106, No. 1, 2002 **191**

(14) Cerdeiriña, C. A.; Míguez, J. A.; Carballo, E.; Tovar, C. A.; de la Puente, E.; Romaní, L. *Thermochim. Acta* **2000**, 347, 37.

(15) (a) Zabransky, M.; Ruzicka, V.; Mayer, V.; Domalski, E. S. *J. Phys. Chem. Ref. Data Monogr.* **1996**, 6. (b) *CDATA: Database of Thermodynamic and Transport Properties for Chemistry and Engineering*; Department of Physical Chemistry. Institute for Chemical Technology (distributed by FIZ Chemie GmbH, Berlin): Prague, 1991.

(16) Troncoso, J.; Carballo, E.; Cerdeiriña, C. A.; González, D.; Romaní, L. *J. Chem. Eng. Data* **2000**, 45, 594.

(17) Marquardt, D. W. *J. Soc. Ind. Appl. Math.* **1963**, 11, 431.

(18) U. de Vigo, CINVESTAV, and UNAM laboratories, unpublished results.

(19) Susuki, S.; Green, P. G.; Bumgarner, R. E.; Dasgupta, S.; Goddard, W. A., III.; Blake, G. A. *Science* **1992**, 257, 942.

(20) Atwood, J. L.; Hamada, F.; Robinson, K. D.; Orr, G. W.; Vincent, R. L. *Nature* **1991**, 349, 683.

(21) Levitt, M.; Perutz, M. W. *J. Mol. Biol.* **1988**, 201, 751.

(22) Costas, M.; Kronberg, B. *Biophys. Chem.* **1998**, 74, 83.